Research Square

Preprints are preliminary reports that have not undergone peer review.
They should not be considered conclusive, used to inform clinical practice,
or referenced by the media as validated information.

TMS Phenotypes of Corticospinal Excitability and Interhemispheric Inhibition in Health and Stroke

Mina Kheirkhah
Philipps University of Marburg
Julia X. Ivanick
University of Southern California
Bardia Rodd
SUNY Upstate Medical University
Yi-Ling Kuo
kuoy@upstate.edu

SUNY Upstate Medical University

Article

Keywords: Corticospinal excitability, Interhemispheric inhibition, Physiological phenotypes, Stroke, Transcranial magnetic stimulation

Posted Date: November 11th, 2026

DOI: https://doi.org/10.21203/rs.3.rs-11587201/v1

License: This work is licensed under a Creative Commons Attribution 4.0 International License.
Read Full License

Additional Declarations: No competing interests reported.

TMS Phenotypes of Corticospinal Excitability and Interhemispheric Inhibition in Health and Stroke

Mina Kheirkhah[1,2], Julia X. Ivanick[3,4], Bardia Rodd[5], Yi-Ling Kuo[6]

1 Department of Psychology, Philipps University of Marburg, Germany.

2 Department of Psychiatry and Psychotherapy, Jena University Hospital, Jena, Germany.

3 USC Caruso Department of Otolaryngology, Keck School of Medicine of USC, University of Southern California, Los Angeles, CA, USA.

4 Department of Stem Cell Biology and Regenerative Medicine, Keck School of Medicine of USC, University of Southern California, Los Angeles, CA, USA.

5 SUNY Upstate Medical University, Syracuse, New York, USA.

6 Department of Physical Therapy Education, SUNY Upstate Medical University, Syracuse, New York, USA.

Corresponding Author: Yi-Ling Kuo

Full address: 3316 Academic Building, 750 East Adams Street, Syracuse, NY 13210, USA

E-mail: kuoy@upstate.edu

Running title: TMS Phenotypes in Health and Stroke

Abstract

Interhemispheric inhibition and corticospinal excitability are widely used biomarkers of motor cortical function. Yet the normative physiological organization of these measures and their relationship to post-stroke dysfunction remain poorly understood. In this cross-sectional observational study, we analyzed bilateral resting motor threshold (rMT) and ipsilateral silent period (iSP) in a large, harmonized cohort of 142 healthy adults to determine whether healthy motor physiology is organized into physiological phenotypes.

Standardized bilateral measures were analyzed using unsupervised clustering. Phenotype structure was further examined using multiple dimensionality-reduction approaches (PR-Isomap, PCA, t-SNE, and UMAP), and supervised classifiers evaluated with repeated stratified 5-fold cross-validation. An independent cohort of 30 individuals with stroke (mean age 65.0 ± 12.8 years; range 40–85; 15 women, 15 men) was then evaluated relative to the fixed healthy-derived reference space without model retraining; 14 participants with complete bilateral measures were eligible for primary four-dimensional projection.

A three-phenotype solution was supported in the healthy cohort: High excitability (51/142), Weak IHI (52/142), and Low excitability (39/142). The phenotypes differed in all four physiological measures (all Kruskal–Wallis $P < 0.0001$) but not in rMT or iSP asymmetry, indicating bilateral physiological differences rather than systematic hemispheric imbalance. Phenotype membership was independent of age, sex, handedness, and musicianship. Phenotype separability was preserved across low-dimensional representations, with mean balanced classification accuracy of approximately 0.90–0.98.

In the projectable stroke subgroup, phenotype distribution differed from that of healthy participants (Monte Carlo $\chi^2(2) = 7.00$, $P = 0.027$, Cramér V = 0.21), with High excitability observed in 10/14 stroke participants (71.4%) compared with 51/142 healthy participants (35.9%). High-excitability assignment was more frequent in stroke (odds ratio = 4.46, 95% confidence interval 1.33–14.95; Fisher's exact $P = 0.018$). In contrast, nearest-centroid distance did not differ between stroke and healthy participants (median 1.54 versus 1.36; U = 1091, $P = 0.550$, Cliff's $\delta = 0.10$). High-excitability enrichment persisted in a sensitivity analysis including 17 stroke participants with at least three of four phenotype-defining measures (11/17, 64.7%; Monte Carlo $P = 0.043$).

These findings demonstrate that healthy motor cortical physiology is organized into reproducible excitability–inhibition phenotypes derived through a multivariate, data-driven framework. Among stroke participants, the principal alteration was redistribution across healthy-derived phenotypes (particularly toward High excitability) rather than global displacement from the healthy phenotype space. Separating phenotype identity from the magnitude of physiological deviation provides a normative framework for interpreting individual post-stroke physiology and may support future biologically informed stratification and precision neuromodulation.

Keywords: Corticospinal excitability; Interhemispheric inhibition; Physiological phenotypes; Stroke; Transcranial magnetic stimulation.

Abbreviations: APB, abductor pollicis brevis; EMG, electromyographic; IHI, interhemispheric inhibition; iSP, ipsilateral silent period; iSP-D, interhemispheric difference in ipsilateral silent period; M1, primary motor cortex; MEP, motor-evoked potential; MSO, maximum stimulator output; rMT, resting motor threshold; rMT-D, interhemispheric difference in resting motor threshold; TMS, transcranial magnetic stimulation; OLS, ordinary least squares; PCA, principal component analysis; PR-Isomap, Parzen-window density isometric mapping; t-SNE, t-distributed stochastic neighbor embedding; UMAP, Uniform Manifold Approximation and Projection; LR, logistic regression; NB, Gaussian naïve Bayes; SVM, support vector machine; RF, random forest. HV, healthy volunteers

Introduction

Interhemispheric interactions between the primary motor cortices (M1) constitute a fundamental organizing principle of the human motor system. Interhemispheric communication is mainly mediated by transcallosal projections, which are predominantly excitatory but can exert a net inhibitory influence on contralateral motor cortical output through local inhibitory circuits.[1–4] This functional interaction, termed interhemispheric inhibition (IHI), can be assessed using transcranial magnetic stimulation (TMS).[4–6] One approach to quantify IHI is the paired-pulse (dual-coil) paradigm, in which a conditioning stimulus delivered to one M1 suppresses the motor-evoked potential (MEP) elicited by a subsequent test stimulus applied to the contralateral M1.[4,6] An alternative single-pulse paradigm is to assess IHI using the ipsilateral silent period (iSP). During voluntary contraction of a target muscle, a suprathreshold TMS pulse delivered to the ipsilateral M1 produces a transient suppression of muscle activity, providing a functional index of transcallosal inhibition. Together, the single-pulse and paired-pulse paradigms are complementary methods for probing interhemispheric motor physiology, although both are sensitive to methodological factors (Hupfeld et al., 2020; Rossini et al., 2015).[7,8] In contrast, some studies have used interhemispheric differences in resting motor threshold (rMT) as an indirect indicator of motor cortical asymmetry. However, rMT primarily reflects corticospinal excitability and does not directly quantify interhemispheric inhibition or connectivity.

In clinical neuroscience, disruption of interhemispheric balance is frequently hypothesized to explain motor impairment after stroke. Excessive inhibitory drive from the intact to the lesioned hemisphere has been documented and interpreted as potentially limiting recovery within the interhemispheric competition models.[9] These models have motivated neuromodulatory interventions aimed at reducing asymmetry, although their effectiveness appears to depend on patient-specific factors, including lesion characteristics and chronicity.[10–14] Yet, such clinical interpretations rest on an implicit assumption: that the healthy motor system is approximately symmetric. However, TMS measures exhibit substantial inter-individual variability arising from physiological fluctuations and methodological factors. This raises the question of whether variability in corticospinal excitability and interhemispheric inhibition reflects identifiable patterns of motor cortical physiology, rather than variation around a single assumed pattern of interhemispheric balance. A multivariate characterization

of bilateral excitability and inhibition may therefore provide information that is not captured by hemispheric asymmetry or single physiological measures considered in isolation.

Despite extensive use of IHI as both a biomarker and a target, fundamental normative questions remain unsettled, in part due to small sample sizes, heterogeneous protocols, and the known variability of TMS measures.[7,15,16] Previous studies have characterized bilateral rMT and IHI and examined their associations with age, handedness, and motor training in healthy cohorts.[15–25] However, these studies have generally examined individual measures, group differences, or demographic associations rather than identifying integrated physiological phenotypes from combined bilateral excitability and inhibition measures. Recent studies have also introduced data-driven phenotyping, patient stratification, and normative-reference approaches in stroke,[26–29] but these frameworks have not derived phenotypes from combined bilateral rMT and IHI in a healthy reference cohort. Moreover, stroke-related alterations in IHI remain heterogeneous across physiological measures and stages of recovery,[30] highlighting the need for a normative reference framework against which pathological motor physiology can be interpreted. Consequently, a large, harmonized normative dataset is needed to define the physiological diversity of the healthy motor system and provide such a reference framework for interpreting pathological alterations after stroke. Applying multivariate, data-driven methods to such a dataset may reveal physiological structure that is obscured by conventional group-average or single-variable approaches.

Against this background, we adopted a multivariate, data-driven machine-learning approach to characterize normative patterns of corticospinal excitability and IHI. Using a large, harmonized dataset of 142 neurologically healthy adults, we analyzed bilateral rMT and iSP, as an index of transcallosal inhibition, to identify latent physiological phenotypes without imposing a priori assumptions regarding hemispheric symmetry or asymmetry. Rather than focusing solely on average hemispheric differences, we investigated whether variability in healthy motor physiology is organized into reproducible phenotypes characterized by distinct combinations of corticospinal excitability and IHI. We further evaluated whether these phenotypes reflected bilateral physiological levels rather than hemispheric imbalance and whether their organization was preserved across complementary low-dimensional representations and classification approaches.

To evaluate the translational relevance of this normative framework, we subsequently projected an independent cohort of individuals with stroke onto the fixed healthy-derived physiological space without retraining the phenotype model. This approach enabled us to determine how

stroke physiology was distributed across healthy-derived phenotypes and whether stroke participants showed greater physiological displacement from the corresponding healthy reference structure. By quantifying each stroke survivor's distance to healthy phenotypic centroids, we further assessed the magnitude of individual physiological deviation independently of phenotype membership. Together, these analyses provide a data-driven normative physiological framework that separates phenotype identity from the magnitude of deviation and enables individual post-stroke physiology to be interpreted relative to the range of configurations observed in health. This framework may ultimately support physiologically informed patient stratification and individualized neuromodulation.

Materials and methods

Participants

Part of the data has been published previously by our group.[18,31–34] A total of 172 participants were included in the study, comprising 142 neurologically healthy adults (mean age = 27.35 ± 7.99 years; range = 18–60 years; 72 males, 70 females) and 30 stroke survivors (mean age = 65.0 ± 12.8 years; range = 40–85 years; 15 males, 15 females). All healthy participants were free of neurological or psychiatric disorders and reported no contraindications to TMS as screened by a TMS safety questionnaire.[35,36] Handedness in the healthy cohort was assessed using the Edinburgh Handedness Inventory[37] (range −100 to +100) and categorized as right-handed (≥ +40; n = 112), mixed-handed (−40 < EHI < +40; n = 14), or left-handed (≤ −40; n = 16). A subset of the healthy participants was classified as professional musicians (n = 73), whose data were derived from our previous studies examining the effects of musicianship on interhemispheric inhibition and hand dexterity.[18,33] The remaining healthy participants were classified as non-musicians (n = 69). In the stroke cohort, lesions predominantly involved vascular territories supplied by the middle cerebral artery, with additional lesions involving pontine, medullary, thalamic, anterior choroidal, and internal carotid artery territories. The affected side was left in 10 participants and right in 20. Missing physiological measurements occurred when reliable responses could not be obtained, including absent ipsilesional MEPs or insufficient voluntary contraction of the paretic hand. Values of rMT coded as 100 in the source dataset denoted that resting motor threshold could not be determined and were therefore treated as unavailable rather than as measured threshold values. Of the 30 stroke participants, 14 had

complete bilateral rMT and iSP measurements and were eligible for the primary analysis. The remaining 16 participants were retained in the stroke cohort for characterization of data availability and projectability but were not used in the primary analysis. Detailed characteristics of this cohort have been reported previously.[34] All procedures were approved by the Institutional Review Board of the SUNY Upstate Medical University (IRB protocol: 1674912) and were conducted in accordance with the Declaration of Helsinki. Written informed consent was obtained from all participants prior to their participation in the study.

Experimental Design and TMS Measurements

Single-pulse TMS was applied over the motor cortical representation of the abductor pollicis brevis (APB) muscle in each M1. In this cross-sectional observational study, the rMT and the iSP were measured and quantified bilaterally using an identical acquisition protocol across all participants. The rMT was defined as the lowest stimulation intensity that elicited a MEP with a peak-to-peak amplitude of at least 50 μV in at least 5 of 10 consecutive trials in the relaxed APB muscle. For the iSP assessment, participants performed approximately 50% of the maximum voluntary contraction of the target muscle while a single suprathreshold stimulus (130% rMT) was delivered over the ipsilateral M1. The magnitude of the iSP was quantified as the percentage suppression of electromyographic (EMG) activity relative to the pre-stimulus contraction level using an objective automated algorithm coded in MATLAB (The MathWorks, Inc., Natick, MA, USA). Detailed iSP acquisition and signal processing methods have been published previously.[32] All TMS data were acquired by the same investigator (Y.L.K.) using identical stimulation procedures (all data were collected using devices from the same brands: TMS: Magstim Co., Whitland, UK; EMG: Motion Lab Systems Inc, Baton Rouge, LA, USA; data acquisition interface: Signal, Cambridge Electronic Design, Cambridge, UK) and processed using the same analysis pipeline, thereby minimizing methodological variability across participants and studies.

In addition to these baseline single-pulse measures, a subset of 74 healthy participants underwent an extended paired-pulse protocol that quantified short- and long-interval IHI during left- and right-hand activation (at approximately 50% maximum muscle contraction, matched to the contraction level during iSP measurements). These measurements were used to examine the relationship between paired-pulse IHI and the interhemispheric differences observed in iSP and rMT. Interstimulus intervals (ISIs) of 10 and 40 ms were used to assess short- and long-interval IHI, respectively.[38,39] In this dual-coil paradigm (with one coil positioned over each

M1), the stimulation intensity required to elicit an approximately 1-mV MEP was used for both the conditioning stimulus (CS) and test stimulus (TS), with intensities determined separately for each hemisphere. Following delivery of the CS to the contralateral M1, the conditioned MEP amplitude elicited by the TS was normalized to the unconditioned baseline MEP amplitude recorded from the same muscle. IHI was then expressed as a percentage: IHI (%) = [1 − (conditioned MEP amplitude / unconditioned MEP amplitude)] × 100. Positive values indicated inhibition, whereas negative values indicated facilitation. The direction of IHI was defined from the hemisphere receiving the CS to the hemisphere receiving the TS (e.g., CS over the left M1 and TS over the right M1 represented left-to-right IHI). Given the distinct dual-coil stimulation paradigm, paired-pulse IHI measures were analyzed separately and excluded from subsequent multivariate analyses. All relevant information is available in the Supplementary Materials (section 1; Supplementary Fig. S1, Supplementary Table S1).

Statistical Analysis, Unsupervised Models, and Classifications

Distributions of rMT and iSP measures of the left hemisphere (rMT-L and iSP-L), right hemisphere (rMT-R and iSP-R), and difference between the right and left hemispheres (rMT-D and iSP-D, calculated as right–left) were tested for normality (Lilliefors, histograms, and Q–Q plots). Hemispheric differences were assessed using paired t-tests or Wilcoxon signed-rank tests as appropriate. The same procedures were applied to absolute asymmetry (|right–left|) and normalized asymmetry indices (AI = (right − left)/(right + left)). Subgroup effects on hemispheric asymmetry (right−left) were tested using unpaired t-tests or Mann–Whitney U tests (sex, musicianship) and ANOVA or Kruskal–Wallis tests (handedness). Associations with age were examined using Pearson's r and Spearman's ρ in the full healthy sample and a ≤40-year subset (N = 135). Ordinary least squares (OLS) and robust regressions (as a sensitivity analysis to reduce the influence of outliers), with age, sex, handedness, and musicianship as predictors, were used to model rMT-D and iSP-D.

Physiological phenotypes were identified by k-means clustering of the four standardized TMS variables (rMT-L, rMT-R, iSP-L, iSP-R). Candidate solutions from K = 2–8 were evaluated using complementary internal-validity and robustness criteria, including silhouette, Davies–Bouldin and Calinski–Harabasz indices, Gap-statistic analysis, repeated subsampling stability, and a sensitivity analysis using bilateral mean rMT and iSP. The final three-cluster solution

was selected on the basis of the combined evidence across these criteria. Physiological characteristics of the resulting phenotypes were compared in the original measurement units using Kruskal–Wallis tests followed by Bonferroni-corrected pairwise Mann–Whitney U tests. Kruskal–Wallis effect sizes were estimated using η^2H.

Phenotype organization based on low-rank approximation was conducted using principal component analysis (PCA)[40,41], Parzen-window density isometric mapping (PR-Isomap)[42], t-distributed stochastic neighbor embedding (t-SNE)[43], and Uniform Manifold Approximation and Projection (UMAP).[44] PR-Isomap was implemented using a k-nearest-neighbour graph followed by a Parzen-window density isometric mapping distance constraint. Candidate parameter combinations were evaluated for graph connectivity and embedding fidelity. The selected solution (k = 15, h = 1.979) yielded a single connected graph while retaining a sparse local neighbourhood structure (graph density = 0.129). Residual variance and reconstruction error for the two-dimensional embedding were 0.102 and 0.251, respectively. For t-SNE, the learning rate was set to auto, with 1000 iterations, perplexity = 30, and random seed = 42. For UMAP, 20 nearest neighbours were used with 400 epochs, min_dist = 0.1, Euclidean distance, and random seed = 42. All embeddings were generated with two components. To assess the separability of the identified phenotypes, supervised classification analyses were performed using four widely used algorithms: logistic regression (LR)[45], Gaussian naïve Bayes (NB)[46], support vector machines (SVM)[47] with a radial basis function kernel, and random forest (RF)[48] classifiers. Classifier performance was evaluated using stratified 5-fold cross-validation (50 permutations), and balanced accuracy was computed to account for unequal class sizes.

Participants with stroke were projected into the four-dimensional standardized physiological space defined by the healthy cohort using the healthy cohort means and standard deviations for bilateral rMT and iSP. Healthy-derived phenotype centroids were kept fixed, and each stroke participant with complete measurements was assigned to the phenotype whose centroid had the smallest Euclidean distance in standardized feature space; clustering was not re-estimated in the stroke cohort. Physiological deviation from the normative phenotype structure was quantified as the Euclidean distance to the nearest healthy phenotype centroid. To provide an unbiased healthy reference distribution for this distance measure, distances in healthy participants were calculated using leave-one-out phenotype centroids. Distances between the projectable stroke subgroup and the healthy reference distribution were compared using the Mann–Whitney U test, with Cliff's delta used as an effect-size measure. Phenotype distributions between healthy and stroke participants were compared using a fixed-margin

Monte Carlo chi-square test, with Cramér's V as the corresponding effect size. A secondary binary analysis compared assignment to the High-excitability phenotype versus the other phenotypes using Fisher's exact test and odds ratios with 95% confidence intervals. Exploratory stroke analyses assessed whether physiological deviation differed by affected side using the Mann–Whitney U test with Cliff's delta and whether phenotype distribution differed by affected side using a fixed-margin Monte Carlo chi-square test. For visualization only, a two-component PCA model was fitted to the healthy standardized data, and stroke participants were transformed into this fixed healthy PCA space without refitting the model.

All statistical analyses were conducted using MATLAB (version R2024a) and Python. All statistical tests were two-sided.

Results

Hemispheric Symmetry of Motor Cortex Excitability and Inhibition

Across the healthy cohort (n = 142), rMTs were comparable between hemispheres (mean ± *SD*: rMT-L = 51.88 ± 10.82 % maximum stimulator output (MSO); rMT-R = 51.14 ± 9.50 %MSO). The mean hemispheric difference (rMT-D) was small (mean ± *SD*: −0.74 ± 7.36 %MSO) and was not statistically significant (paired t-test, P = 0.233), indicating no systematic bias toward either hemisphere. The iSP magnitudes were 46.29 ± 14.90% suppression for iSP-L and 43.99 ± 14.73% for iSP-R. The corresponding hemispheric difference (iSP-D) was −2.30 ± 14.45 percentage EMG suppression and did not reach statistical significance (paired t-test, P = 0.060). Additional details are provided in Supplementary Figs. S2–S3. Overall, cortical excitability and IHI were symmetric on average, but there was a notable inter-individual variability.

Age showed a small positive association with rMT-D (whole healthy cohort: Spearman ρ = 0.202, P = 0.016; participants ≤40 years (N = 135): ρ = 0.194, P = 0.024) and no association with iSP-D (ρ = 0.080, P = 0.384) (see Fig. 1; Supplementary Fig. S4). Consistently, OLS and robust regression analyses again identified age as the only significant predictor of rMT-D (OLS: F = 5.46, P = 0.021; robust: β = 0.198, t = 2.53, P = 0.012), with no significant predictors for iSP-D (Supplementary Tables S2–S3). For rMT-D, no sex differences were observed (t-test P = 0.646, d = −0.08), and no effects of handedness (Kruskal–Wallis P = 0.937, ε^2 = 0.00) or

musicianship (Wilcoxon $P = 0.075$, Cliff's $\delta = -0.17$) were detected. Similarly, iSP-D showed no associations with sex (t-test $P = 0.536$, $d = 0.10$), handedness (ANOVA $P = 0.997$, $\eta^2 = 0.00$), or musicianship (Wilcoxon $P = 0.207$, Cliff's $\delta = 0.12$). Thus, hemispheric asymmetry in rMT and iSP was not systematically explained by sex, handedness, or musicianship, while a modest age-related increase in rMT-D was observed and remained significant after adjustment for these covariates.

Healthy volunteers exhibit distinct TMS phenotypes

Clustering of standardized rMT and iSP measures in 142 healthy volunteers supported retention of a three-cluster solution (K=3). Although the two-cluster solution yielded a marginally higher silhouette coefficient than the three-cluster solution (0.270 vs 0.265), the three-cluster solution was supported by the standard Gap-statistic one-standard-error criterion, greater subsampling stability, improved Davies–Bouldin and Calinski–Harabasz indices relative to $K = 2$, and substantially stronger agreement with a sensitivity analysis based on bilateral mean rMT and iSP (Supplementary Figs. S5–S7 and Supplementary Tables S4–S8). The final three phenotypes comprised 51, 52, and 39 participants, respectively. Together, these complementary analyses supported a reproducible three-cluster partition.

The three phenotypes differed markedly in both rMT and iSP. One phenotype ($n = 51$) was characterized by lower rMT (left 44.96% MSO, right 44.12% MSO) with moderate iSP (left 54.71%, right 50.28%), consistent with increased corticospinal excitability. A second phenotype ($n = 52$) showed intermediate rMT values (left 49.29% MSO, right 50.48% MSO) but markedly reduced iSP values (left 32.41%, right 31.87%), indicating diminished IHI. The third phenotype ($n = 39$) exhibited substantially elevated rMT values bilaterally (left 64.38% MSO, right 61.21% MSO), while iSP values (left 53.80%, right 51.94%) were comparable to those of the high-excitability phenotype, indicating reduced corticospinal excitability (Supplementary Tables S9–S10). Based on the physiological feature that most clearly distinguished each group, the clusters were designated the high excitability phenotype, weak IHI phenotype, and low excitability phenotype, respectively (Fig. 2). These findings suggest that physiological variability in healthy individuals spans partially independent dimensions of corticospinal excitability and interhemispheric inhibitory processing.

All four clustering variables differed significantly across phenotypes (all $P < 0.0001$), with large effect sizes ($\eta^2 = 0.364$–0.530), consistent with distinct physiological profiles across the

three groups (Supplementary Table S10; Fig. 3). Post-hoc analyses showed that bilateral rMT differed significantly between all three phenotypes, whereas iSP primarily distinguished the weak IHI phenotype, which exhibited significantly lower iSP than both the low-excitability and high-excitability phenotypes; iSP did not differ between the latter two phenotypes (Supplementary Table S11). Moreover, no significant differences in interhemispheric asymmetry (right minus left) were observed across phenotypes for either rMT (Kruskal–Wallis $H(2) = 4.69$, $P = 0.096$) or iSP ($H(2) = 1.41$, $P = 0.494$), indicating that the phenotypes differed primarily in overall levels of excitability and inhibition rather than hemispheric imbalance (Supplementary Table S12).

Phenotype membership was not significantly associated with age, sex, handedness, or musicianship (all adjusted $P \geq 0.194$). The handedness result was also unchanged in a permutation-based sensitivity analysis ($P = 0.209$) (Supplementary Table S13). This suggests that the identified phenotypes reflect intrinsic physiological variability rather than sample composition.

Across all embeddings, participants formed visually distinguishable groups that broadly preserved the three healthy-derived phenotype labels. Supervised classification was used to quantify phenotype separability within each fixed two-dimensional representation. Balanced accuracy was highest for PCA (0.939–0.983 across classifiers) and remained high for PR-Isomap (0.948–0.970) and UMAP (0.925–0.946), while t-SNE showed somewhat lower but still substantial performance (0.897–0.908) (Fig. 2 and Supplementary Table S14). These results support the stability and separability of the identified physiological phenotypes across complementary analytical approaches.

Stroke physiology maps onto healthy-derived phenotypes

Of the 30 stroke participants, 14 had complete bilateral rMT and iSP measurements and were therefore eligible for primary projection into the four-dimensional healthy physiological space. Projectability was associated with preservation of an ipsilesional MEP: all 14 projectable participants had a measurable ipsilesional MEP, whereas 7 of the 16 non-projectable participants did not (Fisher's raw $P = 0.007$, Holm-adjusted $P = 0.029$; Supplementary Table S15). Projectability was not associated with age, sex, or lesion side.

Each projectable stroke participant was assigned to the nearest fixed healthy phenotype centroid without retraining the clustering model. The distribution of healthy-derived phenotypes differed between healthy participants and the projectable stroke subgroup (Monte Carlo $\chi^2(2) = 7.00$, $P = 0.027$, Cramér's V=0.21; Fig. 4A-B and Supplementary Tables S16–S17). The High-excitability phenotype predominated after stroke, accounting for 10 of 14 participants (71.4%), compared with 51 of 142 healthy participants (35.9%). Three stroke participants (21.4%) were assigned to the Weak-IHI phenotype and one (7.1%) to the Low-excitability phenotype, compared with 36.6% and 27.5%, respectively, in the healthy cohort (Supplementary Table S18). In a secondary binary analysis, projectable stroke participants had greater odds of assignment to the High-excitability phenotype than healthy participants (odds ratio = 4.46, 95% CI 1.33–14.95; Fisher's exact $P = 0.018$). Projection of individual stroke participants into the healthy PCA representation illustrates that stroke observations largely overlapped the regions occupied by the healthy-derived phenotypes, despite the shift in phenotype frequencies (Fig. 4A).

In a sensitivity analysis including stroke participants with at least three of the four phenotype-defining measures and using only observed standardized dimensions, 17 participants could be classified. The phenotype distribution remained shifted toward the High-excitability phenotype (11/17, 64.7%; Monte Carlo P=0.043), and the secondary High-excitability-versus-other comparison remained significant (odds ratio = 3.27, 95% CI 1.14–9.37; P=0.033) (Supplementary Table S19).

Stroke is associated with phenotype redistribution

Physiological deviation was quantified as distance to the nearest healthy phenotype centroid and compared with a healthy leave-one-out reference distribution. Nearest-centroid distance did not differ between projectable stroke and healthy participants (median 1.54 vs. 1.36; Mann–Whitney U=1091, P=0.550, Cliff's $\delta = 0.10$; Fig. 4C). Only 1/14 stroke participants exceeded the overall healthy 95th-percentile threshold, and 2/14 exceeded phenotype-specific thresholds (Supplementary Table S18C). Thus, among stroke participants with sufficient bilateral physiology for projection, the principal difference from the healthy reference cohort was a redistribution across healthy-derived physiological phenotypes, particularly toward High excitability. Moreover, exploratory analyses suggested greater nearest-centroid distance among participants with right-sided than left-sided lesions (median 1.73 versus 0.90; Mann–Whitney U=6.0, P=0.029, Cliff's $\delta = 0.73$) (Supplementary Table S20).

Discussion

This study establishes a normative physiological reference framework for corticospinal excitability and interhemispheric inhibition between the human motor cortices. To our knowledge, this is the first study with the largest IHI dataset to date to identify discrete physiological phenotypes from combined bilateral TMS-derived cortical measurements and to evaluate stroke physiology within this normative framework. Although previous studies have documented substantial inter-individual variability across TMS measures, they have not examined whether this variability is organized into reproducible physiological states. Our findings demonstrate that healthy motor physiology is structured into discrete excitability–inhibition phenotypes that are largely independent of demographic factors. Among stroke participants with sufficient bilateral physiology for projection, stroke was associated primarily with redistribution across these healthy-derived phenotypes, particularly toward the High-excitability phenotype. Together, these findings suggest that motor cortical physiology is structured into intrinsic configurations that provide a reference for distinguishing normal variability from pathological change.

Normative motor cortical organization

Across a large cohort of healthy adults, corticospinal excitability and IHI were remarkably symmetric at the population level. Neither rMT nor iSP showed a systematic hemispheric bias, suggesting no consistent population-level dominance of one hemisphere over the other, while allowing for marked individual differences in hemispheric asymmetry.[31] However, this symmetry masked considerable inter-individual variability, indicating that normal physiology encompasses a broad range of excitability–inhibition configurations. Age was the only demographic factor associated with hemispheric asymmetry. Increasing age was weakly associated with a more positive right–left rMT difference, whereas no association was observed between age and iSP asymmetry. Previous meta-analytic and empirical studies have reported age-related increases in absolute rMT, consistent with reduced corticospinal excitability.[16,49–51] Age-related changes in iSP and interhemispheric interactions have also been reported, although the specific iSP parameters affected vary across studies and experimental protocols.[7,24,52] Similarly, handedness has been associated with task- and laterality-dependent differences in cortical inhibitory circuitry and transcallosal inhibition,[19,20] whereas findings concerning musicianship and long-term instrumental training have been mixed and appear to

depend on task, instrument, and cortical representation.[18,53,54] In the present pooled cohort, however, sex, handedness, and musicianship were not significantly associated with hemispheric asymmetry. Differences across previous studies may partly reflect variation in sample size and methodology, including stimulation intensity, target muscle, contraction level, and approaches to signal processing and IHI quantification. By pooling a comparatively large dataset acquired and processed using harmonized procedures, the present study was designed to characterize population-level patterns while reducing some of the variability that may have limited earlier smaller studies. These findings indicate that the absence of a systematic population-level hemispheric bias can coexist with substantial inter-individual variability, and that healthy motor cortical organization is better considered as a distribution of physiological configurations rather than a single canonical pattern.

Unsupervised clustering revealed three distinct physiological phenotypes defined by combinations of rMT and iSP. Previous TMS studies have largely examined corticospinal excitability and IHI independently or compared their average values across groups,[15–25] whereas jointly considering these complementary physiological measures revealed reproducible phenotypes that were not apparent from either measure alone. Crucially, these phenotypes differed in absolute levels rather than hemispheric asymmetry, indicating that variability reflects global shifts in motor cortical excitability and inhibition rather than an imbalance between hemispheres. The phenotype structure was therefore driven primarily by bilateral physiological levels rather than interhemispheric differences, highlighting the value of characterizing excitability and inhibition across both hemispheres when defining normative motor cortical phenotypes.

The High-excitability and Low-excitability phenotypes were distinguished primarily by bilateral rMT while showing relatively preserved iSP, whereas the Weak-IHI phenotype was characterized by reduced bilateral iSP with intermediate rMT. This organization suggests that corticospinal excitability and transcallosal inhibition provide partly complementary dimensions of motor-system physiology rather than representing a single physiological axis. The absence of significant demographic associations indicates that phenotype membership was not readily explained by age, sex, handedness, or musicianship in the present cohort. More broadly, the findings suggest that joint variation in excitability and inhibition gives rise to reproducible physiological configurations rather than unstructured inter-individual variability. These healthy-derived phenotypes therefore provide a reference against which post-stroke physiological profiles can be classified and their deviation from healthy physiology quantified.

Stroke within the normative physiological landscape

Projection of the 14 stroke participants with complete bilateral rMT and iSP measurements into the fixed healthy reference space showed that their physiology could be related to the three healthy-derived phenotypes without retraining the clustering model. Earlier TMS studies have demonstrated substantial heterogeneity in corticospinal excitability and IHI after stroke, with findings varying according to the physiological states, chronicity, recovery stage, lesion characteristics, and degree of motor impairment.[11,30,55,56] More recent approaches have therefore sought to stratify stroke populations according to IHI, integrity of the corticospinal tract, clinical impairment, or multivariable physiological profiles.[27,29] In contrast, the present analysis first defined phenotypes in a healthy reference population using combined bilateral rMT and iSP measurements and then evaluated stroke physiology relative to that normative organization.

The principal difference between the healthy cohort and the projectable stroke subgroup was phenotype occupancy. The High-excitability phenotype accounted for 71.4% of projectable stroke participants compared with 35.9% of healthy participants, and the overall phenotype distribution differed significantly between groups. This enrichment was also retained in a sensitivity analysis including participants with at least three of the four phenotype-defining measures. These findings suggest that stroke may alter the probability of occupying particular regions of the healthy-derived physiological landscape rather than necessarily generating a qualitatively distinct physiological configuration. This interpretation is strengthened by the centroid-distance analysis. The projectable stroke subgroup was not globally farther from the healthy phenotype centroids than healthy participants themselves. Nearest-centroid distance was similar between groups, and only a small number of stroke participants exceeded the healthy 95th-percentile reference thresholds. Thus, the dominant group-level effect was redistribution across healthy-derived phenotypes rather than generalized displacement from them. This distinction between phenotype occupancy and distance from the corresponding normative centroid may help explain why conventional group-mean studies can yield heterogeneous findings:[30,56] individuals may occupy different physiological configurations despite showing similar overall degrees of deviation from a healthy reference.

An important qualification is that primary four-dimensional projection was possible for only 14 of the 30 acute stroke participants. Projectability was strongly associated with preservation of an ipsilesional MEP, indicating that the primary projected subgroup was enriched for

individuals with preserved ipsilesional corticospinal responsiveness and potentially greatermotor recovery capasity.[57] However, given that the stroke phenotype distribution is highly biased toward the High excitability phenotype regardless of fully obtainable phenotype-defining measures (bilateral rMT and iSP), acute post-stroke cortical responsiveness phenotype may be independent of the predictability of motor recovery. The observed phenotype frequencies therefore should not be interpreted as representative of the entire stroke cohort. Rather, they characterize the subset in whom bilateral rMT and iSP could be reliably quantified.

In an exploratory analysis, participants with right-sided lesions showed greater nearest-centroid distance than those with left-sided lesions (Cliff's $\delta \approx 0.73$), suggesting a potentially sizeable laterality-related difference in physiological deviation. However, this finding was based on only five left- and nine right-lesion participants and should therefore be considered hypothesis-generating rather than evidence of a robust hemispheric effect. Centroid distance is also a physiological measure and should not be interpreted as an index of clinical severity. Previous studies have reported lesion-side-related differences in motor-network organization and post-stroke phenotypes, but the direction and biological basis of such effects remain uncertain.[5,9,28] Whether the observed difference in our study reflects hemispheric specialization, lesion characteristics, sampling variability, or differences in transcallosal organization will require confirmation in substantially larger cohorts. We therefore avoid concluding that lesion hemisphere determines phenotype membership or produces a systematic direction of physiological reorganization.

Implications for neuromodulation and rehabilitation

Traditional models of stroke recovery often emphasize pathological interhemispheric imbalance, particularly excessive inhibition from the contralesional hemisphere.[11] Accordingly, it is commonly used in neurorehabilitation to up-regulate the affected hemisphere and down-regulate the unaffected one via cortical stimulation.[58] The present findings support a more heterogeneous view. The healthy motor system itself comprises multiple excitability–inhibition configurations, and the projectable stroke subgroup was redistributed across these configurations rather than uniformly displaced into a single abnormal physiological state.

In practical terms, this raises the possibility that interventions could eventually be informed by both an individual's physiological phenotype and their continuous deviation from the

corresponding healthy reference, rather than assuming a common pattern of contralesional hyperinhibition across patients. Although this concept requires prospective validation, a normative phenotype framework may provide a foundation for more individualized neuromodulation strategies. However, the present study does not test treatment response and therefore cannot establish that phenotype-guided stimulation improves clinical outcomes. Prospective studies linking physiological phenotype, centroid distance, motor impairment, recovery trajectories, and response to neuromodulation will be necessary before this framework can be used clinically. In summary, understanding the full range of normative physiological variability with bilateral comprehensive examinations of corticospinal excitability and transcallosal inhibition is essential for interpreting post-stroke pathophysiology and may facilitate more personalized rehabilitation strategies.

Limitations and future directions

Several limitations should be acknowledged. First, the stroke cohort was relatively small, and only 14 of 30 participants had complete bilateral rMT and iSP measurements for the primary four-dimensional projection. However, the main finding was supported by a sensitivity analysis including participants with at least three of the four phenotype-defining measures, increasing the analyzable sample to 17 and yielding a similar enrichment of the High-excitability phenotype. In a separate sensitivity analysis treating undetermined rMT values coded as 100 as numerical ceiling values, the direction of the association was also preserved, although the effect was attenuated and no longer statistically significant (High excitability vs. other phenotypes: OR = 2.97, P=0.056; overall phenotype distribution P=0.111) (Supplementary Table S19). Nevertheless, because projectability was associated with preserved ipsilesional MEPs, the primary findings should be interpreted as most applicable to stroke participants with measurable bilateral corticospinal physiology. Second, the healthy reference cohort was substantially younger than the stroke cohort, and relatively few healthy participants were within the age range of the stroke group. Consequently, we were unable to perform a sufficiently powered sensitivity analysis restricted to age-matched or older healthy participants. Although phenotype membership was not significantly associated with age in the healthy cohort, this does not exclude age-related effects on the continuous resting motor threshold and ipsilateral silent-period measures. Accordingly, the observed difference in phenotype frequencies between healthy and stroke participants may partly reflect age differences in addition to stroke-related physiology. Future studies should validate this framework using an age-matched

healthy reference cohort or age-adjusted normative models. Last, the cross-sectional design cannot determine whether the identified physiological phenotypes represent stable traits or dynamic states. Future studies should examine longitudinal changes, their relationship with motor behavior and functional recovery, and whether physiological phenotyping can inform individualized neuromodulation and rehabilitation strategies.

Conclusion

In conclusion, this study provides a normative physiological framework for interpreting motor cortical excitability and IHI. By applying a data-driven, machine-learning approach to a large pooled dataset of bilateral TMS measurements, we characterized the distribution of healthy motor physiology without imposing predefined physiological categories and identified reproducible patterns that would not be apparent from conventional group-average analyses alone. Rather than representing a single physiological state, healthy motor cortex organization comprises discrete excitability–inhibition phenotypes defined by distinct combinations of bilateral corticospinal excitability and transcallosal inhibition. The additional projection of an independent stroke cohort onto this fixed healthy-derived reference space extends this framework from physiological characterization to individualized interpretation of disease-related physiology. Among stroke participants with measurable bilateral physiology, the principal difference from the healthy reference was a redistribution across these phenotypes (particularly toward High excitability) rather than a generalized increase in distance from healthy phenotype centroids.

More broadly, this study illustrates how multivariate data-science approaches can move TMS research beyond single-measure and group-average comparisons by jointly modelling multiple dimensions of motor-system physiology and positioning individual patients relative to the physiological variation observed in health. These findings demonstrate the value of separating phenotype identity from the magnitude of individual physiological deviation and provide a framework for interpreting post-stroke motor physiology relative to the range of configurations observed in health. Validation in larger, age-matched and longitudinal cohorts will be required to determine the clinical and therapeutic relevance of this normative approach.

Data availability

The datasets analysed during the current study are available from the corresponding author on reasonable request, subject to institutional policies and participant confidentiality requirements.

Funding

This work was partly supported by the Eunice Kennedy Shriver National Institute of Child Health and Human Development (NICHD), National Institutes of Health (R03HD123642), and the Research: Art Works Grant, National Endowment for the Arts (NEA) (17-3800-7002).

Competing interests

The authors report no competing interests.

Supplementary material

Supplementary material is available at *Brain* online.

References

1. Genç E, Ocklenburg S, Singer W, Güntürkün O. Abnormal interhemispheric motor interactions in patients with callosal agenesis. *Behavioural Brain Research*. 2015;293:1-9. doi:10.1016/j.bbr.2015.07.016

2. Hofer S, Frahm J. Topography of the human corpus callosum revisited—Comprehensive fiber tractography using diffusion tensor magnetic resonance imaging. *NeuroImage*. 2006;32(3):989-994. doi:10.1016/j.neuroimage.2006.05.044

3. Ruddy KL, Leemans A, Carson RG. Transcallosal connectivity of the human cortical motor network. *Brain Struct Funct*. 2017;222(3):1243-1252. doi:10.1007/s00429-016-1274-1

4. Daskalakis ZJ, Christensen BK, Fitzgerald PB, Roshan L, Chen R. The mechanisms of interhemispheric inhibition in the human motor cortex. *The Journal of Physiology*. 2002;543(1):317-326. doi:10.1113/jphysiol.2002.017673

5. Carson RG. Inter-hemispheric inhibition sculpts the output of neural circuits by co-opting the two cerebral hemispheres. *The Journal of Physiology*. 2020;598(21):4781-4802. doi:10.1113/JP279793

6. Ferbert A, Priori A, Rothwell JC, Day BL, Colebatch JG, Marsden CD. Interhemispheric inhibition of the human motor cortex. *The Journal of Physiology*. 1992;453(1):525-546. doi:10.1113/jphysiol.1992.sp019243

7. Hupfeld KE, Swanson CW, Fling BW, Seidler RD. TMS-induced silent periods: A review of methods and call for consistency. *Journal of Neuroscience Methods*. 2020;346:108950. doi:10.1016/j.jneumeth.2020.108950

8. Rossini PM, Burke D, Chen R, et al. Non-invasive electrical and magnetic stimulation of the brain, spinal cord, roots and peripheral nerves: Basic principles and procedures for routine clinical and research application. An updated report from an I.F.C.N. Committee. *Clinical Neurophysiology*. 2015;126(6):1071-1107. doi:10.1016/j.clinph.2015.02.001

9. Di Pino G, Pellegrino G, Assenza G, et al. Modulation of brain plasticity in stroke: a novel model for neurorehabilitation. *Nat Rev Neurol*. 2014;10(10):597-608. doi:10.1038/nrneurol.2014.162

10. Boddington LJ, Reynolds JNJ. Targeting interhemispheric inhibition with neuromodulation to enhance stroke rehabilitation. *Brain Stimulation*. 2017;10(2):214-222. doi:10.1016/j.brs.2017.01.006

11. Murase N, Duque J, Mazzocchio R, Cohen LG. Influence of interhemispheric interactions on motor function in chronic stroke. *Annals of Neurology*. 2004;55(3):400-409. doi:10.1002/ana.10848

12. Plow EB, Cunningham DA, Varnerin N, Machado A. Rethinking Stimulation of the Brain in Stroke Rehabilitation: Why Higher Motor Areas Might Be Better Alternatives for Patients with Greater Impairments. *Neuroscientist*. 2015;21(3):225-240. doi:10.1177/1073858414537381

13. Sung WH, Wang CP, Chou CL, Chen YC, Chang YC, Tsai PY. Efficacy of Coupling Inhibitory and Facilitatory Repetitive Transcranial Magnetic Stimulation to Enhance Motor Recovery in Hemiplegic Stroke Patients. *Stroke*. 2013;44(5):1375-1382. doi:10.1161/STROKEAHA.111.000522

14. Dodd KC, Nair VA, Prabhakaran V. Role of the Contralesional vs. Ipsilesional Hemisphere in Stroke Recovery. *Front Hum Neurosci*. 2017;11:469. doi:10.3389/fnhum.2017.00469

15. Beaulieu LD, Flamand VH, Massé-Alarie H, Schneider C. Reliability and minimal detectable change of transcranial magnetic stimulation outcomes in healthy adults: A systematic review. *Brain Stimulation*. 2017;10(2):196-213. doi:10.1016/j.brs.2016.12.008

16. Bhandari A, Radhu N, Farzan F, et al. A meta-analysis of the effects of aging on motor cortex neurophysiology assessed by transcranial magnetic stimulation. *Clinical Neurophysiology*. 2016;127(8):2834-2845. doi:10.1016/j.clinph.2016.05.363

17. Hanlon CA, McCalley DM. Sex/Gender as a Factor That Influences Transcranial Magnetic Stimulation Treatment Outcome: Three Potential Biological Explanations. *Front Psychiatry*. 2022;13:869070. doi:10.3389/fpsyt.2022.869070

18. Kuo YL, Kutch JJ, Fisher BE. Relationship between Interhemispheric Inhibition and Dexterous Hand Performance in Musicians and Non-musicians. *Sci Rep*. 2019;9(1):11574. doi:10.1038/s41598-019-47959-y

19. Davidson T, Tremblay F. Hemispheric Differences in Corticospinal Excitability and in Transcallosal Inhibition in Relation to Degree of Handedness. Balasubramaniam R, ed. *PLoS ONE*. 2013;8(7):e70286. doi:10.1371/journal.pone.0070286

20. Reid CS, Serrien DJ. Handedness and the excitability of cortical inhibitory circuits. *Behavioural Brain Research*. 2012;230(1):144-148. doi:10.1016/j.bbr.2012.02.008

21. Rosenkranz K, Williamon A, Rothwell JC. Motorcortical Excitability and Synaptic Plasticity Is Enhanced in Professional Musicians. *J Neurosci*. 2007;27(19):5200-5206. doi:10.1523/JNEUROSCI.0836-07.2007

22. Davidson T, Tremblay F. Age and hemispheric differences in transcallosal inhibition between motor cortices: an ispsilateral silent period study. *BMC Neurosci*. 2013;14(1):62. doi:10.1186/1471-2202-14-62

23. Wiemann M, Drämel N, Madsen MAJ, et al. Influence of stimulus intensity on the TMS induced ipsilateral silent period – Comprehensive findings from a large healthy cohort. *Clinical Neurophysiology*. 2026;184:2111588. doi:10.1016/j.clinph.2026.2111588

24. Coppi E, Houdayer E, Chieffo R, et al. Age-Related Changes in Motor Cortical Representation and Interhemispheric Interactions: A Transcranial Magnetic Stimulation Study. *Front Aging Neurosci*. 2014;6. doi:10.3389/fnagi.2014.00209

25. Ciechanski P, Zewdie E, Kirton A. Developmental profile of motor cortex transcallosal inhibition in children and adolescents. *Journal of Neurophysiology*. 2017;118(1):140-148. doi:10.1152/jn.00076.2017

26. Takechi U, Matsunaga K, Nakanishi R, et al. Longitudinal changes of motor cortical excitability and transcallosal inhibition after subcortical stroke. *Clinical Neurophysiology*. 2014;125(10):2055-2069. doi:10.1016/j.clinph.2014.01.034

27. Lin YL, Potter-Baker KA, Cunningham DA, et al. Stratifying chronic stroke patients based on the influence of contralesional motor cortices: An inter-hemispheric inhibition study. *Clinical Neurophysiology*. 2020;131(10):2516-2525. doi:10.1016/j.clinph.2020.06.016

28. De Doncker W, Kuppuswamy A. Lesioned hemisphere-specific phenotypes of post-stroke fatigue emerge from motor and mood characteristics in chronic stroke. *Euro J of Neurology*. 2024;31(3):e16170. doi:10.1111/ene.16170

29. Shanks MJ, Cirillo J, Stinear CM, Byblow WD. A novel TMS framework for assessing neurophysiological recovery at the subacute stage after stroke. *Clinical Neurophysiology*. 2025;171:82-94. doi:10.1016/j.clinph.2025.01.010

30. Gerges ANH, Hordacre B, Pietro FD, Moseley GL, Berryman C. Do Adults with Stroke have Altered Interhemispheric Inhibition? A Systematic Review with Meta-Analysis. *Journal of Stroke and Cerebrovascular Diseases*. 2022;31(7):106494. doi:10.1016/j.jstrokecerebrovasdis.2022.106494

31. Kuo YL, Arroyo DF, Carrier R, Madonna E. Is Interhemispheric Inhibition Balanced between the Two Primary Motor Cortices? A Large-scale Analysis. *Brain Stimulation: Basic, Translational, and Clinical Research in Neuromodulation*. 2023;16(1):354. doi:10.1016/j.brs.2023.01.684

32. Kuo YL, Dubuc T, Boufadel DF, Fisher BE. Measuring ipsilateral silent period: Effects of muscle contraction levels and quantification methods. *Brain Research*. 2017;1674:77-83. doi:10.1016/j.brainres.2017.08.015

33. Kuo YL, Fisher BE. Relationship between interhemispheric inhibition and bimanual coordination: absence of instrument specificity on motor performance in professional musicians. *Exp Brain Res*. 2020;238(12):2921-2930. doi:10.1007/s00221-020-05951-3

34. Kuo YL, Lin DJ, Vora I, DiCarlo JA, Edwards DJ, Kimberley TJ. Transcranial magnetic stimulation to assess motor neurophysiology after acute stroke in the United States: Feasibility, lessons learned, and values for future research. *Brain Stimulation*. 2022;15(1):179-181. doi:10.1016/j.brs.2021.12.001

35. Rossi S, Antal A, Bestmann S, et al. Safety and recommendations for TMS use in healthy subjects and patient populations, with updates on training, ethical and regulatory issues: Expert Guidelines. *Clinical Neurophysiology*. 2021;132(1):269-306. doi:10.1016/j.clinph.2020.10.003

36. Rossi S, Hallett M, Rossini PM, Pascual-Leone A. Safety, ethical considerations, and application guidelines for the use of transcranial magnetic stimulation in clinical practice and research. *Clinical Neurophysiology*. 2009;120(12):2008-2039. doi:10.1016/j.clinph.2009.08.016

37. Oldfield RC. The assessment and analysis of handedness: the Edinburgh inventory. *Neuropsychologia*. 1971;9(1):97-113.

38. Chen R, Yung D, Li JY. Organization of Ipsilateral Excitatory and Inhibitory Pathways in the Human Motor Cortex. *Journal of Neurophysiology*. 2003;89(3):1256-1264. doi:10.1152/jn.00950.2002

39. Ni Z, Gunraj C, Nelson AJ, et al. Two Phases of Interhemispheric Inhibition between Motor Related Cortical Areas and the Primary Motor Cortex in Human. *Cerebral Cortex*. 2009;19(7):1654-1665. doi:10.1093/cercor/bhn201

40. Jolliffe IT. Principal component analysis: a beginner's guide—I. Introduction and application. *Weather*. 1990;45(10):375-382.

41. Abdi H, Williams LJ. Principal component analysis. *WIREs Computational Stats*. 2010;2(4):433-459. doi:10.1002/wics.101

42. Yousefi B, Khansari M, Trask R, et al. Measuring Subtle HD Data Representation and Multimodal Imaging Phenotype Embedding for Precision Medicine. *IEEE Trans Instrum Meas*. 2025;74:1-11. doi:10.1109/TIM.2025.3545983

43. Van der Maaten L, Hinton G. Visualizing data using t-SNE. *Journal of machine learning research*. 2008;9(11).

44. McInnes L, Healy J, Melville J. UMAP: Uniform Manifold Approximation and Projection for Dimension Reduction. *arXiv*. Preprint posted online 2018. doi:10.48550/ARXIV.1802.03426

45. Hosmer DW, Lemeshow S, Sturdivant RX. *Applied Logistic Regression*. Wiley; 2013. https://books.google.de/books?id=bRoxQBIZRd4C

46. Murphy KP. *Machine Learning: A Probabilistic Perspective*. MIT press; 2012.

47. Cortes C, Vapnik V. Support-vector networks. *Mach Learn*. 1995;20(3):273-297. doi:10.1007/BF00994018

48. Breiman L. Random Forests. *Machine Learning*. 2001;45(1):5-32. doi:10.1023/A:1010933404324

49. Rossini PM, Desiato MT, Caramia MD. Age-related changes of motor evoked potentials in healthy humans: Non-invasive evaluation of central and peripheral motor tracts excitability and conductivity. *Brain Research*. 1992;593(1):14-19. doi:10.1016/0006-8993(92)91256-E

50. Cuypers K, Thijs H, Duque J, Swinnen SP, Levin O, Meesen RLJ. Age-related differences in corticospinal excitability during a choice reaction time task. *AGE*. 2013;35(5):1705-1719. doi:10.1007/s11357-012-9471-1

51. Levin O, Cuypers K, Netz Y, et al. Age-related differences in human corticospinal excitability during simple reaction time. *Neuroscience Letters*. 2011;487(1):53-57. doi:https://doi.org/10.1016/j.neulet.2010.09.072

52. Petitjean M, Ko JYL. An age-related change in the ipsilateral silent period of a small hand muscle. *Clinical Neurophysiology*. 2013;124(2):346-353. doi:10.1016/j.clinph.2012.07.006

53. Chieffo R, Straffi L, Inuggi A, et al. Motor Cortical Plasticity to Training Started in Childhood: The Example of Piano Players. Cattaneo L, ed. *PLoS ONE*. 2016;11(6):e0157952. doi:10.1371/journal.pone.0157952

54. Izbicki P, Mendoza T, Zaman A, Stegemöller EL. Differences in motor inhibition in young and older musicians and non-musicians at rest. *Front Aging Neurosci*. 2023;15:1230865. doi:10.3389/fnagi.2023.1230865

55. McDonnell MN, Stinear CM. TMS measures of motor cortex function after stroke: A meta-analysis. *Brain Stimulation*. 2017;10(4):721-734. doi:10.1016/j.brs.2017.03.008

56. Bütefisch CM, Weβling M, Netz J, Seitz RJ, Hömberg V. Relationship Between Interhemispheric Inhibition and Motor Cortex Excitability in Subacute Stroke Patients. *Neurorehabil Neural Repair*. 2008;22(1):4-21. doi:10.1177/1545968307301769

57. Jordan H, Norrie O, Stinear CM. The Accuracy of the PREP2 Prediction Tool for Upper Limb Outcomes After Stroke as Part of Routine Clinical Care. *Neurorehabil Neural Repair*. 2026;40(3):235-245. doi:10.1177/15459683251412283

58. Safdar A, Smith MC, Byblow WD, Stinear CM. Applications of Repetitive Transcranial Magnetic Stimulation to Improve Upper Limb Motor Performance After Stroke: A Systematic Review. *Neurorehabil Neural Repair*. 2023;37(11-12):837-849. doi:10.1177/15459683231209722

Figures

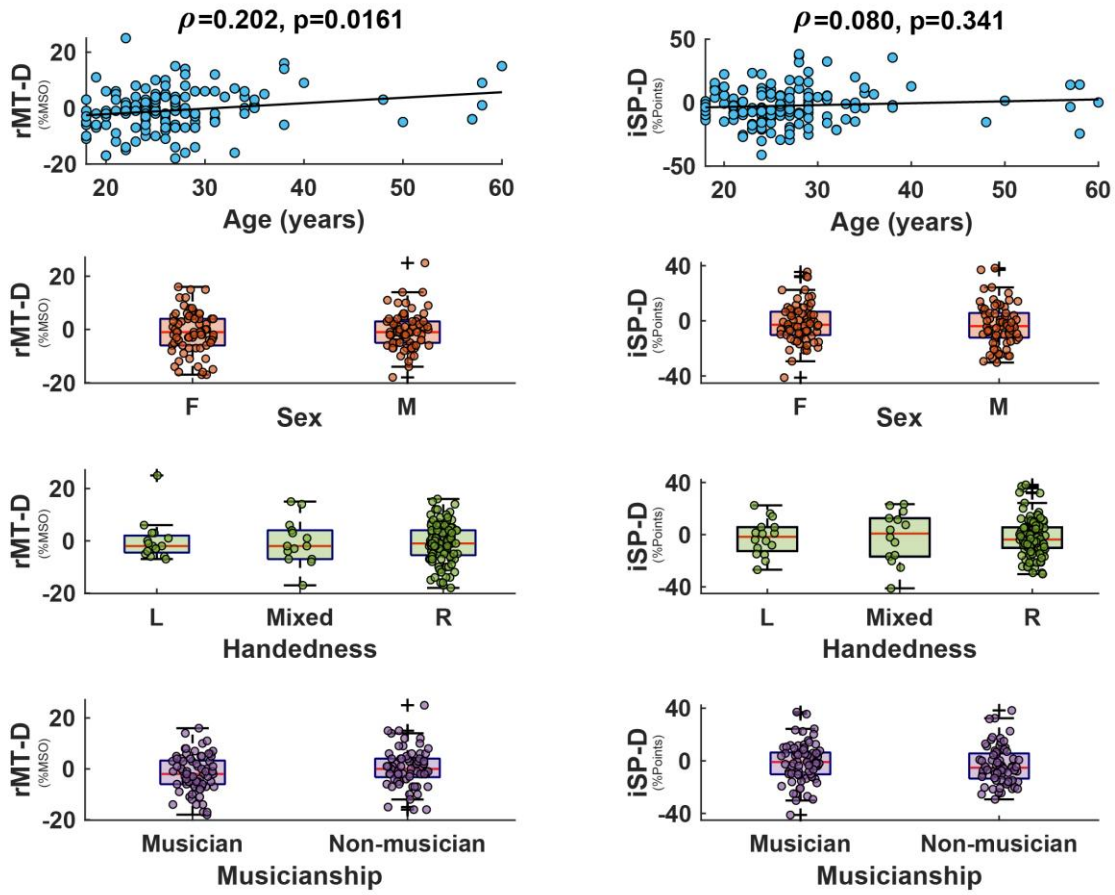


Figure 1. Interhemispheric asymmetry in corticospinal excitability (rMT-D) and inhibition (iSP-D) with subgroup analyses in the healthy sample (N = 142). *First row:* Associations of age with rMT-D (Right–Left, %MSO) and iSP-D (Right–Left, % points), shown as scatterplots with least-squares regression lines. Spearman correlation coefficients (ρ) and corresponding P values are displayed. Age was weakly positively associated with rMT-D, whereas no significant association was observed between age and iSP-D. *Rows 2–4:* Distributions of rMT-D (*left*) and iSP-D (*right*) according to sex, handedness, and musicianship, shown as boxplots with individual data points overlaid. Positive right–left values indicate greater values for the right than the left hemisphere, whereas negative values indicate greater values for the left hemisphere. Overall, these findings indicate substantial inter-individual variability in hemispheric asymmetry but little evidence that this variability is explained by demographic or behavioral factors, with the exception of a modest positive association between age and rMT-D. This age result is unchanged when excluding participants >40 y (Supplementary Fig. S4).

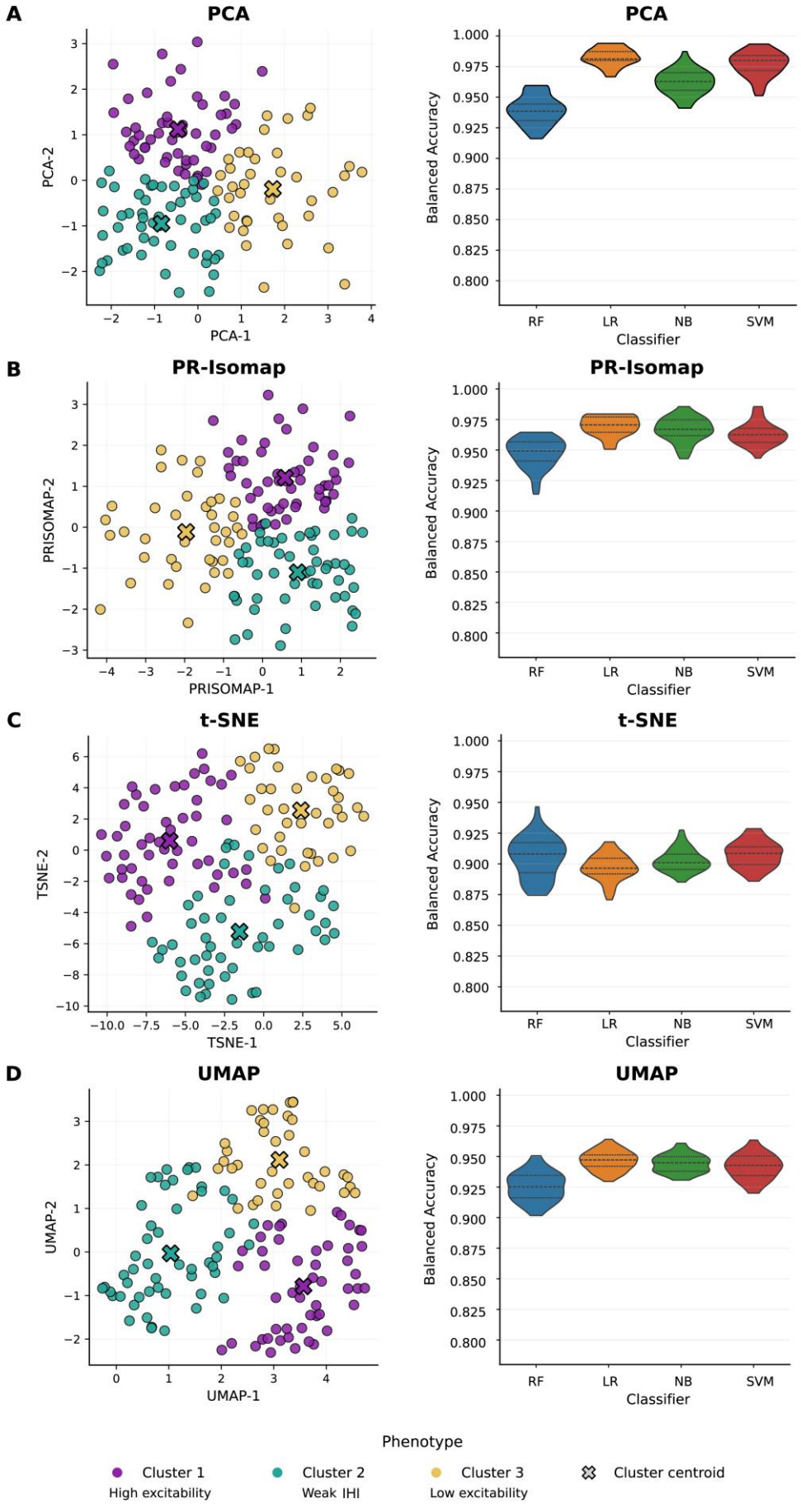

A
PCA
PCA-2
PCA-1
PCA
Balanced Accuracy
RF
LR
NB
SVM
Classifier
B
PR-Isomap
PRISOMAP-2
PRISOMAP-1
PR-Isomap
Balanced Accuracy
RF
LR
NB
SVM
Classifier
C
t-SNE
TSNE-2
TSNE-1
t-SNE
Balanced Accuracy
RF
LR
NB
SVM
Classifier
D
UMAP
UMAP-2
UMAP-1
UMAP
Balanced Accuracy
RF
LR
NB
SVM
Classifier
Phenotype
Cluster 1
High excitability
Cluster 2
Weak IHI
Cluster 3
Low excitability
Cluster centroid

Figure 2. Low-dimensional representation and separability of healthy-derived physiological phenotypes. Three physiological phenotypes derived from standardized bilateral resting motor threshold (rMT, %MSO) and ipsilateral silent period (iSP, % points) measures were visualized across four two-dimensional embeddings: **(A)** principal component analysis (PCA), **(B)** Parzen-window density isometric mapping (PR-Isomap), **(C)** t-distributed stochastic neighbour embedding (t-SNE), and **(D)** Uniform Manifold Approximation and Projection (UMAP). In the *left* column, individual healthy participants are coloured according to their phenotype assignment: High excitability (Cluster 1, purple), Weak IHI (Cluster 2, teal), and Low excitability (Cluster 3, yellow); crosses indicate phenotype centroids in each embedding. In the *right* column, violin plots show the distribution of balanced classification accuracy for predicting the fixed phenotype labels from each two-dimensional embedding using random forest (RF), logistic regression (LR), Gaussian naïve Bayes (NB), and support vector machine (SVM) classifiers across repeated stratified cross-validation. Phenotype separation was preserved across all four representations, with the highest classification performance generally observed for PCA and PR-Isomap and lower, although still substantial, performance for t-SNE.

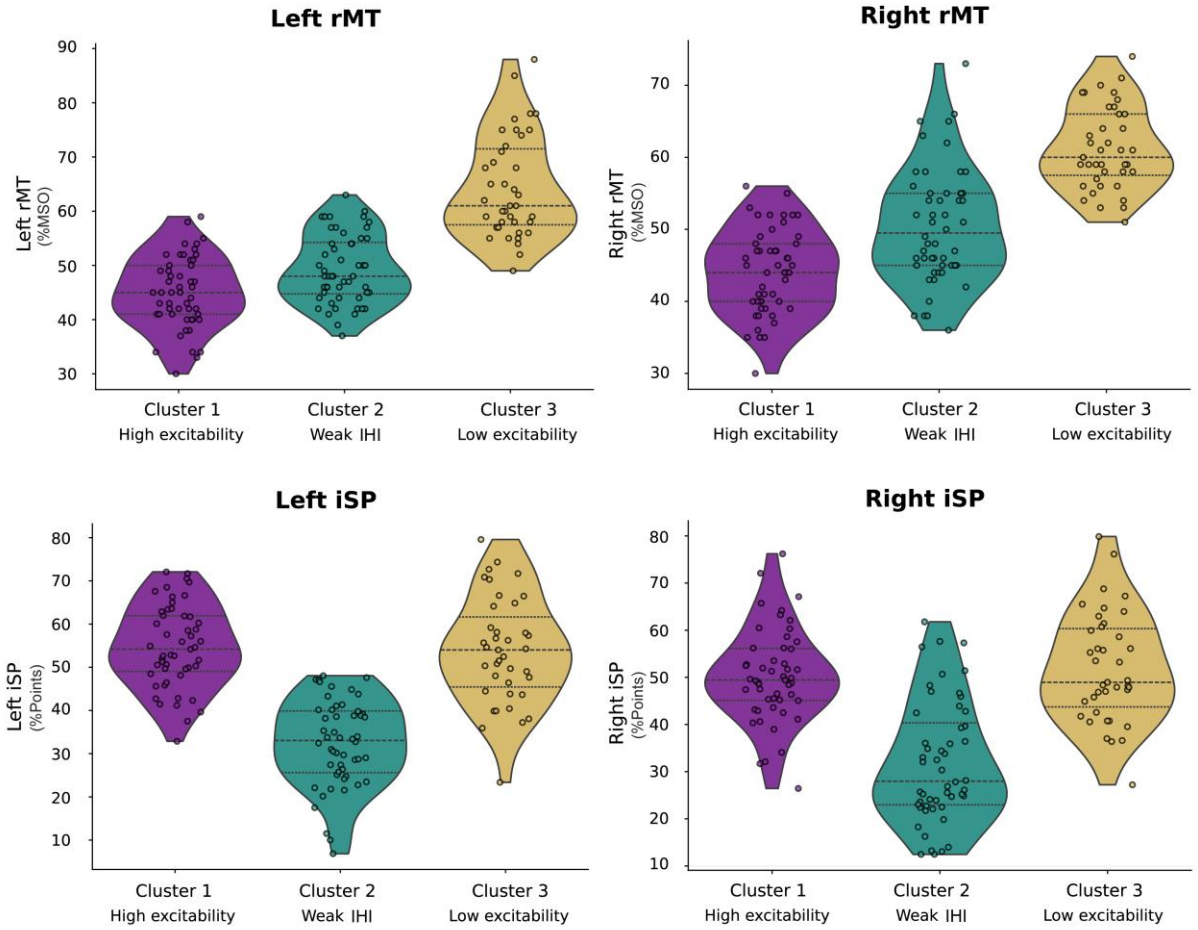


Figure 3. Physiological characteristics of the three healthy-derived TMS phenotypes. Violin plots show the distributions of resting motor threshold (rMT) and ipsilateral silent period (iSP) for the left and right hemispheres across the three phenotypes identified in the healthy cohort: High excitability, Weak IHI, and Low excitability. Individual participants are shown as overlaid points, with internal dashed lines indicating the median and interquartile range.

Lower rMT values indicate greater corticospinal excitability, whereas higher iSP values indicate stronger interhemispheric inhibition. The High-excitability phenotype was characterized by low bilateral rMT with relatively preserved iSP, the Weak-IHI phenotype by reduced bilateral iSP with intermediate rMT, and the Low-excitability phenotype by high bilateral rMT with relatively preserved iSP. All four physiological measures differed significantly across phenotypes (Kruskal–Wallis tests, all $P<0.0001$); pairwise comparisons are provided in the Supplementary Materials.

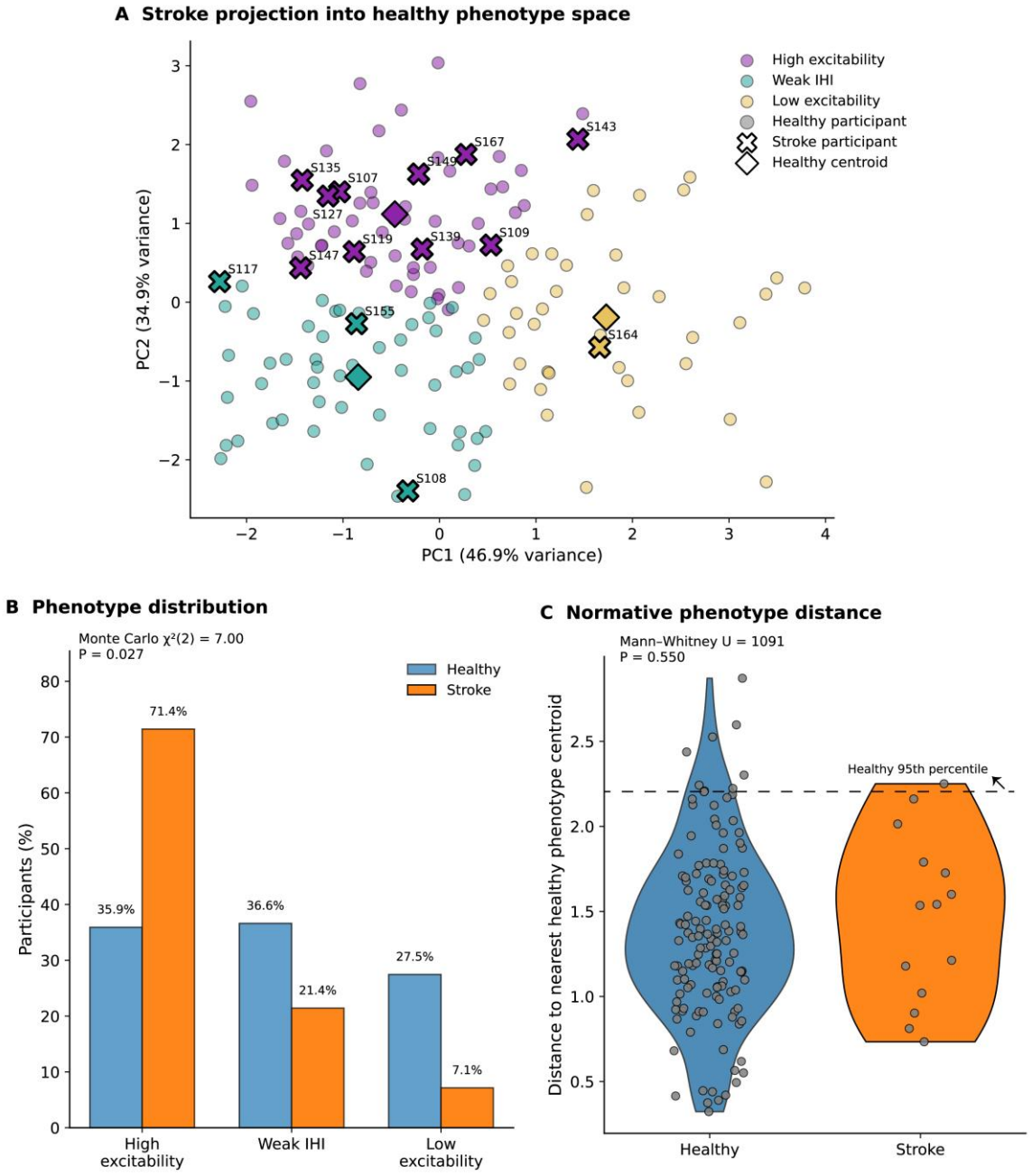


Figure 4. Projection of stroke physiology onto healthy-derived physiological phenotypes. **(A)** Two-dimensional PCA visualization of the standardized healthy physiological space defined by bilateral resting motor threshold (rMT) and ipsilateral silent period (iSP). Healthy

participants are shown according to their three healthy-derived phenotypes, with the 14 stroke participants having complete four-dimensional physiological data superimposed as larger symbols. PCA was used for visualization only; stroke phenotype assignment was performed by nearest-centroid classification in the original standardized four-dimensional feature space. **(B)** Distribution of healthy-derived phenotypes in healthy participants and the primary projectable stroke subgroup. Phenotype distributions differed between groups (fixed-margin Monte Carlo $\chi^2(2) = 7.00$, P=0.027), with a greater proportion of stroke participants assigned to the High-excitability phenotype. **(C)** Distribution of distance to the nearest healthy phenotype centroid in healthy participants, calculated using leave-one-out centroids, and in projectable stroke participants. Nearest-centroid distance did not differ between groups (Mann–Whitney U=1091, P=0.550). The dashed line indicates the 95th percentile of the healthy leave-one-out distance distribution.

Supplementary Files

This is a list of supplementary files associated with this preprint. Click to download.

- KheirkhahetalSupplementaryMaterials.docx